

# Spontaneous generation of persistent activity in diffusively coupled cellular assemblies

Ria Ghosh<sup>1,2</sup> and Shakti N. Menon<sup>1</sup>

<sup>1</sup>*The Institute of Mathematical Sciences, CIT Campus, Taramani, Chennai 600113, India*

<sup>2</sup>*Homi Bhabha National Institute, Anushaktinagar, Mumbai 400 094, India*

(Dated: September 27, 2021)

The spontaneous generation of electrical activity underpins a number of essential physiological processes, and is observed even in tissues where specialized pacemaker cells have not been identified. The emergence of periodic oscillations in diffusively coupled assemblies of excitable and electrically passive cells (which are individually incapable of sustaining autonomous activity) has been suggested as a possible mechanism underlying such phenomena. In this paper we investigate the dynamics of such assemblies in more detail by considering simple motifs of coupled electrically active and passive cells. The resulting behavior encompasses a wide range of dynamical phenomena, including chaos. However, embedding such assemblies in a lattice yields spatio-temporal patterns that either correspond to a quiescent state or partial/globally synchronized oscillations. The resulting reduction in dynamical complexity suggests an emergent simplicity in the collective dynamics of such large, spatially extended systems. Furthermore, we show that such patterns can be reproduced by a reduced model comprising only excitatory and oscillatory elements. Our results suggest a generalization of the mechanism by which periodic activity can emerge in a heterogeneous system comprising non-oscillatory elements by coupling them diffusively, provided their steady states in isolation are sufficiently dissimilar.

Spontaneously recurring electrical activity is of crucial significance in a number of physiological contexts [1–3]. This is typically driven by pacemaker cells [4–6], such as the sinoatrial node in the heart which comprises specialized cells that periodically generate signals initiating excitatory activity, leading to mechanical contraction [7]. However, such cells have not been observed in other contractile tissue, such as the myometrium of the gravid uterus [8]. It has been hypothesized that spontaneous activity in the latter contexts arise through interactions between electrically active and passive cells, local assemblies of which are capable of generating periodic waves of activation in the tissue through diffusive coupling [9, 10]. These waves traveling through an organ are capable of sustaining spatio-temporally coherent contractions [11]. Indeed it has been demonstrated that one of the simplest ways to achieve this is by having an excitable cell coupled by gap-junctions to one (or more) electrically passive cells characterized by a resting state membrane potential that is much higher than that of the excitable cell [12]. The coupling between these heterogeneous cell types causes the membrane potential of the excitable cell to be driven beyond its threshold, resulting in the generation of an action potential. Subsequently, the excitable cell attempts to return to its resting state, but after a period of recovery is again driven to exceed its threshold by the passive cells coupled to it, thereby resulting in a periodically recurring series of action potentials. Thus, although neither excitable nor passive cells are individually capable of spontaneous sustained activation, an assembly of these two cell types can generate periodic oscillations [13].

The emergence of periodic activity in a heterogeneous assembly of excitable and passive cells makes such a mechanism a viable candidate for self-organized system-wide coherent oscillations in physiological contexts where

no pacemakers have been reported [14, 15]. Indeed, it has been demonstrated that a lattice of excitable cells that are each coupled to a variable number of passive cells, can exhibit a range of spatio-temporal phenomena consistent with those observed in the uterus during the transition to coherent activity seen prior to parturition [11, 16, 17]. However, noting that each local cellular assembly are either in an excitable or an oscillatory dynamical regime in isolation, raises an important question: can the observed collective behavior be reproduced in an even simpler setting, viz., where each lattice site is occupied by either an oscillatory or an excitable element, a situation reminiscent of percolation [18]. In this paper, we consider the dynamics of two classes of systems, each capable of exhibiting spontaneous collective dynamics, one comprising electrically active and passive cells (EP) and the other comprising oscillatory and excitable cells (OE). We observe that simple motifs of cells described using the EP model are capable of exhibiting a wide range of complex collective dynamical patterns. However, several of these are no longer observed when such cells are embedded in a spatially extended system, suggesting an emergent simplicity of the collective dynamics. More importantly, we observe that when cells described by the OE model are placed on a lattice, the resulting dynamics are qualitatively very similar to that obtained using the EP model. This points towards a more fundamental mechanism that could explain the emergence of spontaneous recurrent activity in physiologically relevant contexts.

To investigate in detail the range of complex behavior that emerges upon diffusively coupling excitable cells, each of which are in turn coupled to one or more passive cells, we consider the simplest possible assemblies of these cells capable of exhibiting spontaneous oscillatory activity. Following Ref. [11], we simulate the electrical

arXiv:2109.11837v1 [nlin.AO] 24 Sep 2021

activity of an excitable cell using the FitzHugh-Nagumo (FHN) model [19], which is capable of both excitable and oscillatory dynamics. The model describes the temporal evolution of an activation variable  $V_e$  (the membrane potential), and an inactivation variable  $g$  (an effective trans-membrane conductance) as  $\dot{V}_e = \mathcal{F}(V_e, g)$ ,  $\dot{g} = \mathcal{G}(V_e, g)$ . Here,  $\mathcal{F}(V_e, g) = AV_e(V_e - \alpha)(1 - V_e) - g$  and  $\mathcal{G}(V_e, g) = \epsilon(k_e V_e - g - b)$ , where  $A(= 3)$  and  $k_e(= 1)$  govern the kinetics,  $\alpha(= 0.2)$  is the excitation threshold and  $\epsilon(= 0.08)$  is the recovery rate, while  $b$  provides a measure of the asymmetry of the limit cycle. We note that for  $b_{c1}(= 0.127) < b < b_{c2}(= 0.343)$  the cell exhibits periodic oscillations, while outside this range it is excitable with a stable resting state. The value of  $V_e$  in the resting state is close to 0 for  $b < b_{c1}$  and consequently this regime is characterized as a “low” stable state. For  $b > b_{c2}$ , the resting state value of  $V_e$  is relatively large, with the regime being referred to as a “high” stable state. The temporal evolution of the passive cell is described in terms of its membrane potential  $V_p$  as  $\dot{V}_p = K(V_p^R - V_p)$ , where  $V_p^R(= 1.5)$  is the resting state and  $K(= 0.25)$  is the relaxation rate [20]. Each excitable cell is electrically coupled to  $n_p(= 0, 1, 2, \dots)$  passive cells, where the conductance of the gap junctions between the two cell types is  $C_r$ . Thus, the set of equations used to describe the dynamics of an excitable cell  $i$  coupled to  $n_p^i$  passive cells, as well as to an excitable cell  $j$ , is:

$$\begin{aligned} \frac{dV_e^i}{dt} &= \mathcal{F}(V_e^i, g^i) + n_p^i C_r (V_p^i - V_e^i) + D(V_e^j - V_e^i), \\ \frac{dg^i}{dt} &= \mathcal{G}(V_e^i, g^i), \\ \frac{dV_p^i}{dt} &= K(V_p^R - V_p^i) - C_r(V_p^i - V_e^i). \end{aligned} \quad (1)$$

The dynamics of an isolated excitable cell coupled to one or more passive cells depends on  $n_p$  and  $C_r$ . As  $V_p^R$  is much higher than the excitation threshold  $\alpha$ , for a range of  $n_p$  and  $C_r$  the coupled excitable-passive system can exhibit oscillations. To demonstrate that such emergent oscillations result exclusively from the coupling we have chosen  $b = 0$ , so that in isolation the FHN dynamics converges to the low stable state. It is important to note in the context of the results reported here that when  $C_r > 0.5$ , oscillations are seen only for  $n_p = 1$  while those excitable cells coupled to  $n_p > 1$  passive cells converge to high stable states. We first consider the simplest non-trivial assembly of dissimilar excitable-passive units, viz., a pair of excitable cells diffusively coupled with strength  $D$ , each interacting with a different number  $n_p$  of passive cells with strength  $C_r$  (Fig. 1). The heterogeneity in  $n_p$  implies that the intrinsic behavior of the two units are dissimilar, and we observe a range of distinct collective dynamics upon varying  $D$  and  $C_r$ , as shown in Fig. 1 (a-d) for four distinct connection topologies of the assemblies [illustrated in the top right corners of the corresponding panels]. The dynamical regimes obtained can

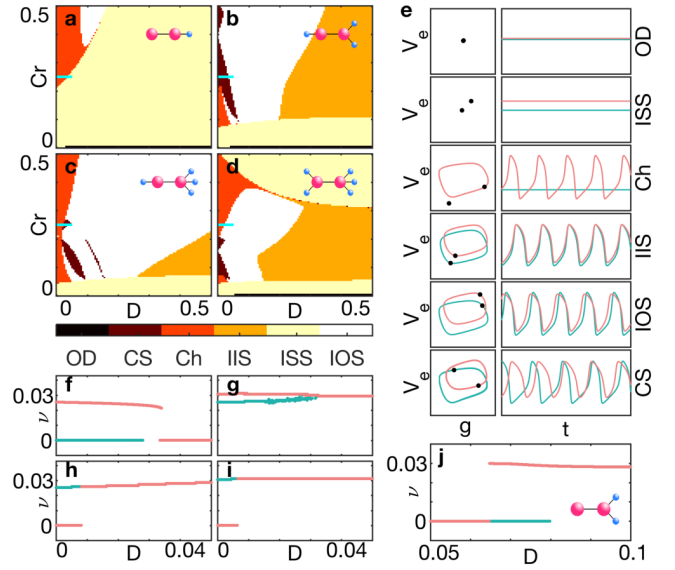


FIG. 1. **Emergent dynamics obtained with different motifs of diffusively coupled excitable and passive cells.** (a-d) Collective dynamical patterns observed over a range of values of diffusive coupling strengths between two excitable cells ( $D$ ) and between an excitable and a passive cell ( $C_r$ ), obtained using different motifs (shown as insets in the corresponding panels, where the larger and smaller circles represent excitable and passive cells, respectively). The regimes are classified according to the dominant attractor obtained for the given parameter set, and include oscillation death (OD), inhomogeneous steady state (ISS), chimera (Ch), inhomogeneous in-phase synchronization (IIS), inhomogeneous out-of-phase synchronization (IOS) and cluster synchronization (CS). (e) Phase plane trajectories and time series of the excitable cells for the different collective dynamical regimes displayed in (a-d). The black dots represent the instantaneous position of the two cells on the corresponding limit cycle. (f-i) Variation of the frequency  $\nu$  of the excitable cells on the left (green) and right (maroon) in each of the four motifs in (a-d) for  $C_r = 0.25$ , over the range of  $D$  indicated by horizontal cyan bars in (a-d). As  $D$  increases, frequencies of the two cells merge and for sufficiently strong coupling the system can either stop oscillating (f), or display a frequency that is between (g), greater than (h) or equal to (i) the maximum of the intrinsic frequencies. (j) Variation of  $\nu$  with  $D$  for  $C_r = 0.6$ , obtained using the motif shown as an inset. Although both cells are quiescent for low coupling strength, they exhibit oscillations for sufficiently large  $D$ .

be classified on the basis of the  $V_e$  time-series of the excitable cells, using a set of order parameters with specified threshold values (see SI for details): (i) oscillation death (OD), where both cells are in the same temporally invariant non-zero steady state; (ii) inhomogeneous steady state (ISS), where both cells are in different temporally invariant steady states; (iii) chimera (Ch), where only one of the two cells oscillate; (iv) inhomogeneous in-phase synchronization (IIS), where both cells oscillate in-phase; (v) inhomogeneous out-of-phase synchroniza-

tion (IOS), where both cells have the same frequency but are out-of-phase with each other, and, (vi) cluster synchronization (CS), where the two cells have different oscillation frequencies [Fig. 1 (e)]. At low values of  $D$ , the two units can behave very differently, and we observe collective states such as Ch or CS. As  $D$  increases, the cells either become frequency locked or cease oscillating altogether. Note that the intrinsic heterogeneity of the two units prevents exact synchronization between them even for large  $D$ . For a given value of  $D$ , as  $C_r$  is decreased, eventually the cells stop oscillating (in isolation, neither an excitable nor a passive cell is capable of spontaneous activity).

In Fig. 1 (f-i), we display the variation of the frequency  $\nu$  of the periodic activity exhibited by the excitable cells in the low  $D$  regime in each of the different assemblies ( $C_r$  is fixed at 0.25 in each case). We observe that an increase in  $D$  either gives rise to the cessation of oscillations [Fig. 1(f)] or a synchronized state in which the two units oscillate at a common frequency that is either lower [Fig. 1(g)], higher [Fig. 1(h)] or equal to [Fig. 1(i)] the higher of the pair of intrinsic frequencies (i.e., the frequencies of each unit at  $D = 0$ ). Just as coupling an excitable cell to one or more passive cells can, under appropriate conditions, give rise to oscillatory dynamics, we observe that spontaneous activity can arise upon coupling a pair of dissimilar units that do not oscillate in isolation. Fig. 1 (j) shows a pair of excitable cells, having  $n_p = 0$  and  $n_p = 2$  respectively, such that neither can independently oscillate for  $C_r = 0.6$ . However, upon increasing  $D$  sufficiently, we observe a transition to a Ch state and eventually to a frequency synchronized state of the two units.

Upon increasing the number of units in an assembly, we observe that the system becomes capable of exhibiting more complex collective behavior including chaotic activity. However, a particularly intriguing collective state of coexisting chaotic and non-chaotic activity is observed in an assembly of three excitable cells, having  $n_p = 1, 2, 3$  respectively, that are coupled in a chain [see top right corner of Fig. 2 (a)]. For a large range of values of  $C_r$  and  $D$ , the system exhibits IOS [Fig. 2 (a)]. However, in the CS regime, we observe a collective dynamical state that is characterized by chaotic behavior in the excitable cell with  $n_p = 1$  with non-chaotic, periodic oscillations in the other two cells [Fig. 2 (b-d)] The qualitative difference in the dynamics of the three excitable cells is evident upon comparing their time series [Fig. 2(b)], phase plane portraits [Fig. 2(c)] and power spectral densities [Fig. 2(d)]. A more rigorous comparison, considering the response of each cell to small perturbations, shows rapid divergence of the resulting trajectory from the unperturbed one for the chaotic unit, with no such deviation observed for the other two units (see SI). We note that permutations of the connection topology of this assembly, i.e. changing the order in which the cells with different values of  $n_p$  are

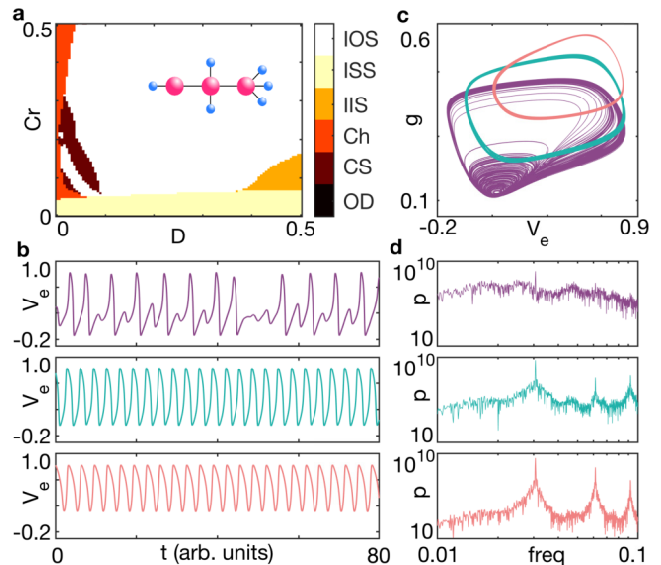


FIG. 2. **Coexistence of chaotic and non-chaotic dynamical activity in a system of three diffusively coupled excitable cells, each coupled to a different number ( $n_p$ ) of passive cells.** (a) Collective dynamical patterns observed over a range of values of diffusive coupling strengths  $D$  between excitable cells and the coupling  $C_r$  between excitable and passive cells for the system shown as an inset. The dynamical regimes are classified according to the dominant attractor obtained for the given parameter set, and are the same as those detailed in Fig. 1 (a-d). (b) Time series of membrane potential  $V_e$  of the excitable cells coupled to (top)  $n_p = 1$ , (middle)  $n_p = 2$  and (bottom)  $n_p = 3$  passive cells, for  $D = 0.02$  and  $C_r = 0.19$ . (c-d) Phase plane trajectories and power spectral densities of the three excitable cells, colored as in the corresponding panels of (b).

placed in the chain, yields similar qualitative behavior, with chaotic dynamics consistently observed in the unit with the lowest  $n_p$ .

It may appear that increasing the size of the assemblies further, by adding more coupled excitable-passive units, can only lead to a further increase in the complexity of the collective dynamics. However, surprisingly, we observe an *emergent simplicity* in the behavior of large lattices of such units, with neighboring elements coupled diffusively to each other. Indeed, such an example is provided by a spatially extended model of uterine tissue, which is heterogeneous by nature, comprising electrically active myocytes that are excitable (thereby facilitating muscle contractions), as well as electrically passive cells such as interstitial Cajal-like cells (ICLC) [21] and fibroblasts [see top panel of Fig. 3 (a)]. The system exhibits spontaneous oscillations for a range of values of  $C_r$  even though, in isolation, none of the individual cells are capable of autonomous periodic activity, as has been experimentally observed in uterine tissue [14, 15]. More important from the perspective of the dynamical transition

to periodic coordinated contraction of the myometrium, it is seen that increasing  $D$  results in the self-organized emergence of global synchronization, and eventually coherence [11, 17]. It is striking that such coordination is achieved exclusively through local interactions between cells and does not require a centralized pacemaker such as that present in the heart (viz., the sino-atrial node).

The relative simplicity of the collective behavior of such a lattice of heterogeneous coupled cells can be shown by demonstrating that it can be captured by a reduced description of the system in terms of interacting dynamical elements, each of which are either in an oscillating or a steady state. In particular, we can replace excitable-passive cell assemblies that are capable of spontaneous periodic activation by a single FHN unit with  $b_{c1} < b < b_{c2}$  (for concreteness, we choose  $b_{osc} = 0.192$  for the simulations whose results are shown here), and FHN units with  $b < b_{c1}$  ( $> b_{c2}$ ) for cell assemblies exhibiting a low (high) stable state (we choose  $b_{exc}^{low} = 0$  and  $b_{exc}^{high} = 0.394$  for the simulations shown here). The resulting equivalent lattice now comprises only FHN units, a fraction  $f$  of which are in an oscillatory regime with the remaining being excitable by virtue of having different values of  $b$  [see Fig. 3 (a), bottom panel]. Nevertheless, the system exhibits qualitatively identical behavior to that seen in models of uterine tissue simulated by coupling assemblies of excitable and passive elements, e.g., the occurrence of cluster synchronization at relatively low inter-cellular coupling that gives way to global synchronization of periodic activity (coordinated by propagating waves of excitation that traverse the lattice) for stronger coupling [Fig. 3 (b)].

The similarity of the emergent properties of the simpler model can be established further by comparing the different dynamical regimes of the  $f - D$  parameter space with that observed in the uterine model having heterogeneous cell types [11]. Indeed all the qualitatively distinct types of behavior reported in the latter can be seen in Fig. 3 (c), including No Oscillation (NO, with all cells in steady states), Cluster Synchronization (CS, marked by coexistence of multiple groups of cells, each characterized by a different frequency), Local Synchronization (LS, coexistence of quiescent cells with cells oscillating at a common frequency), Global Synchronization (GS, all cells have the same oscillation frequency) and Coherence (COH, all cells exhibit phase synchrony). In the limit of large  $D$ , the dynamics of lattice can be further simplified and an implicit analytical equation can be obtained for  $f_c$ , the fraction of FHN units that should be oscillatory for the system to exhibit persistent periodic excitations. It marks the boundary between the NO and COH regimes and is given as  $b_{c1} = (1 - f_c) b_{exc} + f_c b_{osc}$ . For the situation shown in Fig. 3 (c),  $b_{exc} = b_{exc}^{low}$ , which yields  $f_c \sim 0.7$  upon inserting the corresponding numerical values.

We can investigate the collective dynamics around this

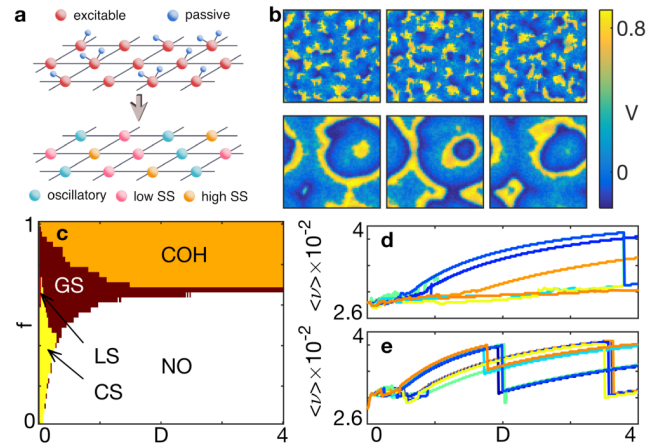


**FIG. 3. Collective dynamics of a lattice of diffusively coupled elements that can be either excitable or oscillatory.** (a) Schematic diagram of uterine tissue, modeled as a two-dimensional lattice where each site comprises an excitable cell coupled to a variable number of passive cells (top, the “EP” model). The dynamics at each site can equivalently be described through cells that are either oscillatory or excitable (bottom, the “OE” model). The latter cell type could be in one of two possible steady states, characterized by low and high values of the state variable  $V$ . Note that the number of passive cells coupled to each excitable cell in the top panel is chosen such that the uncoupled dynamics at that site is qualitatively the same as that of the corresponding site in the bottom panel. (b) Snapshots of the activity  $V$  in a planar simulation domain comprising an equal mixture of excitable and oscillatory elements ( $f = 0.5$ ) diffusively coupled with strength  $D$  to nearest neighbors, showing (top row,  $D = 0.1$ ) cluster synchronization (CS) and (bottom row,  $D = 0.3$ ) global synchronization (GS). (c) Varying the diffusion coefficient  $D$  and the fraction of oscillatory cells  $f$  in the lattice for the case of the OE model, several distinct dynamical regimes are observed. In addition to CS and GS, these include local synchronization (LS), coherence (COH) and no oscillations (NO). The regions are identified according to the collective dynamics observed for the majority ( $> 50\%$ ) of initial conditions. (d-e) Variation of the mean oscillatory frequency  $\langle \nu \rangle$  with  $D$ . Each curve is obtained by starting from different random initial states at low  $D$  and then gradually increasing  $D$  over time. In panel (d), the cell at each site can be either oscillatory (with probability  $f = 0.7$ ) or excitable (with probability  $1 - f$ ). In panel (e), we first associate with each lattice site a random number  $n$  drawn from a Poisson distribution (with mean  $\lambda = 0.7$ ), and then place oscillatory cells in sites with  $n = 1$  and excitable cells having a low or high  $V$  steady states at sites with  $n = 0$  and  $n > 1$ , respectively. All simulations are performed on square lattices comprising  $64 \times 64$  cells, with periodic boundary conditions.

asymptotic boundary between persistent oscillatory activity and a quiescent steady state by considering the case  $f = 0.7$ . In particular, we focus on the variation of the overall activation rate, measured by the mean frequency of periodic activation  $\langle \nu \rangle$  (averaged over all oscil-

lating elements in the lattice), as  $D$  is increased. In order to be consistent with the physiological setting, where the coupling between cells increases over the gestation period (as a result of hormone induced increased expression of gap junctions that electrically couple the cells [22]),  $D$  is increased adiabatically over the course of a single realization, from a random initial condition at a low value of  $D$ . For the situation when  $b_{exc} = b_{exc}^{low}$ , shown in Fig. 3 (d),  $\langle \nu \rangle$  increases with  $D$  until it reaches a maximum value related to the reciprocal of the refractory period (set by the parameters of the FHN model). Increasing  $D$  further results in an abrupt drop in  $\langle \nu \rangle$  as the number of propagating wavefronts in the system changes. A subsequent increase in  $D$  results in an increase in  $\langle \nu \rangle$  generated by the new spatio-temporal pattern. This is qualitatively the same as the phenomenon observed for the model of uterine tissue involving assemblies of excitable and passive cells. An even closer match between the two classes of models can be obtained if we replace each of the excitable elements with FHN elements having either  $b_{exc} = b_{exc}^{low}$  or  $b_{exc}^{high}$  according to the following procedure: first, each lattice site is assigned a value  $n$  chosen from a Poisson distribution with mean  $\lambda = f$ . Note that this is identical to the process by which the number of passive cells (given by  $n$ ) coupled to an excitable cell are determined in modeling uterine tissue with excitable-passive cell assemblies [11]. Next, FHN units in the oscillatory regime ( $b = b_{osc}$ ) are placed at sites having  $n = 1$ , while FHN units with  $b = b_{exc}^{low}$  (i.e., excitable element with a low stable state) are placed at sites with  $n = 0$ . At sites having  $n > 1$ , corresponding to excitable-passive cell assemblies whose activity is arrested at a high stable state, FHN units with  $b = b_{exc}^{high}$  are placed. The resulting oscillatory-excitable (OE) model can accurately reproduce dynamical behaviors reported for the model comprising excitable-passive (EP) cell assemblies [11]. These include the emergence of clusters characterized by a common oscillation frequency, propagating wavefronts, as well as self-sustained spiral waves in the GS regime [see SI for details]. Note that persistent periodic activity can arise upon coupling two FHN units that cannot independently oscillate, provided one of them is in the low and the other in the high stable state - a phenomenon analogous to the appearance of oscillations in assemblies of excitable and passive cells which cannot sustain autonomous activity. Fig. 3 (e) shows the evolution of the mean frequency with  $D$  when the cellular coupling is increased adiabatically starting from a random initial condition over the course of a single realization, displaying an even closer agreement to the behavior seen in the EP model of uterine tissue [11].

The qualitative equivalence of the collective behavior in large lattices for the two classes of models is all the more surprising as the dynamics of network motifs comprising excitable-passive cell assemblies (discussed above, see Figs. 1 and 2) is much more complex than that ob-

served upon replacing each assembly by a FHN unit in the oscillatory or excitable regime. For instance, coupling a pair of EP cell assemblies, each of which oscillate at different frequencies, cannot give rise to exact synchronization even at large  $D$ . However, two FHN oscillators characterized by distinct  $b$  values (and hence, frequencies) can exhibit exact synchronization when coupled with sufficient strength. Furthermore, while we have reported motifs of connected EP cell assemblies that exhibit chimera (Ch) regimes over a range of coupling strengths, such behavior cannot be seen in two coupled FHN oscillators with distinct intrinsic frequencies. We would also like to point out that nothing equivalent to the chaotic behavior observed in a motif comprising coupled EP cell assemblies (Fig. 2) is seen in systems of coupled FHN oscillators arranged in a similar topology (viz., a chain comprising two oscillators having different intrinsic frequencies and an excitable element). Thus, even though the OE model reproduces the collective behavior of a large system of coupled EP cell assemblies, the dynamics at the microscopic level (i.e., motifs comprising only a few elements) can be extremely different for the two classes of models (see SI).

To conclude, in this paper we have shown that while coupled excitable-passive cell assemblies are capable of exhibiting a wide range of dynamical behaviors including chaos, a macroscopic system comprising a large number of such elements diffusively coupled to their nearest neighbors on a lattice shows relatively simpler spatio-temporal phenomena. In particular, this resulting collective dynamics can be reproduced by a model comprising many elements, each described by a generic model for an excitable cell that is either in a steady state or in an oscillatory regime. Indeed, it suggests that the behavior associated with physiologically detailed models of uterine tissue activity [16, 17, 23] can be understood in terms of a reduced model involving a heterogeneous assembly of coupled oscillatory and excitable elements. More importantly, our results point towards a generalization of the mechanism proposed in Ref. [12] for the emergence of periodic activity in systems where none of the individual elements are intrinsically capable of oscillating. While it was shown there that persistent oscillations arise upon coupling excitable and electrically passive cells under certain circumstances, here we have shown that an oscillating system may emerge upon coupling elements, each of which are in isolation at time-invariant steady states - provided these states are dissimilar (i.e., the state variables associated with them have sufficiently distinct numerical values, corresponding to “low” and “high”). Furthermore, our demonstration of a large variety of dynamical attractors in small assemblies of excitable and passive elements can provide an understanding of the complex dynamics seen in electrically coupled heterogeneous sub-cellular compartments in neurons [24, 25] and small networks of neurons interacting via gap-junctions [26].

We would like to thank Sitabhra Sinha and K. A. Chandrashekar for helpful discussions. SNM has been supported by the IMSc Complex Systems Project (12th Plan), and the Center of Excellence in Complex Systems and Data Science, both funded by the Department of Atomic Energy, Government of India. The simulations and computations required for this work were supported by the Institute of Mathematical Sciences High Performance Computing facility (hpc.imsc.res.in) [Nandadevi and Satpura clusters].

- 
- [1] L. Glass, *Nature (London)* **410**, 277 (2001). doi:10.1038/35065745
- [2] M. I. Rabinovich, P. Varona, A. I. Selverston, and H. D. Abarbanel, *Rev. Mod. Phys.* **78**, 1213 (2006). doi:10.1103/RevModPhys.78.1213
- [3] S. Sinha and S. Sridhar, *Patterns in Excitable Media: Genesis, Dynamics, and Control*, (CRC Press, Boca Raton, FL, 2015).
- [4] J. D. Huizinga, L. Thuneberg, M. Klüppel, J. Malysz, H. B. Mikkelsen, and A. Bernstein, *Nature (Lond.)* **373**, 347 (1995). doi:10.1038/373347a0
- [5] L. Thomson, T. L. Robinson, J. C. F. Lee, L. A. Farraway, M. J. G. Hughes, D. W. Andrews, and J. D. Huizinga, *Nat. Med.* **4**, 848 (1998). doi:10.1038/nm0798-848
- [6] J. D. Huizinga *et. al.*, *Nat. Commun.* **5**, 3326 (2014). doi:10.1038/ncomms4326
- [7] M. R. Boyett, H. Honjo, and I. Kodama, *Cardiovasc. Res.* **47**, 658 (2000). doi:10.1016/S0008-6363(00)00135-8
- [8] R. Smith, M. Imtiaz, D. Banney, J. W. Paul, and R. C. Young, *Am. J. Obstet. Gynecol.* **213**, 181 (2015). doi:10.1016/j.ajog.2015.06.040
- [9] J. H. E. Cartwright, *Phys. Rev. E* **62**, 1149 (2000). doi:10.1103/PhysRevE.62.1149
- [10] C. Degli Esposti Boschi, E. Louis, and G. Ortega, *Phys. Rev. E* **65**, 012901 (2001). doi:10.1103/PhysRevE.65.012901
- [11] R. Singh, J. Xu, N. B. Garnier, A. Pumir, and S. Sinha, *Phys. Rev. Lett.* **108**, 068102 (2012). doi:10.1103/PhysRevLett.108.068102
- [12] V. Jacquemet, *Phys. Rev. E* **74**, 011908 (2006). doi:10.1103/PhysRevE.74.011908
- [13] T. A. Quinn, P. Camelliti, E. A. Rog-Zielinska, U. Siedlecka, T. Poggioli, E. T. O'Toole, T. Knöpfel, and P. Kohl, *Proc. Natl. Acad. Sci. USA* **113**, 14852 (2016). doi:10.1073/pnas.1611184114
- [14] S. Wray, S. Kupittayanant, A. Shmygol, R. D. Smith, and, T. Burdyga, *Exp. Physiol.* **86**, 239 (2001). doi:10.1113/eph8602114
- [15] R. C. Young, *Best Pract. Res. Clin. Obstet. Gynaecol.* **52**, 68 (2018). doi:10.1016/j.bpobgyn.2018.04.002
- [16] J. Xu, S. N. Menon, R. Singh, N. B. Garnier, S. Sinha, and A. Pumir, *PLoS ONE* **10**, e0118443 (2015). doi:10.1371/journal.pone.0118443
- [17] J. Xu, R. Singh, N. B. Garnier, S. Sinha, and A. Pumir, *New J. Phys.* **15**, 093046 (2013). doi:10.1088/1367-2630/15/9/093046
- [18] D. Stauffer and A. Aharony, *Introduction to Percolation Theory*, (CRC Press, Boca Raton, FL, 1994).
- [19] J. Keener and J. Sneyd, *Mathematical Physiology*, (Springer, New York, 1998).
- [20] P. Kohl, A. G. Kamkin, I. S. Kiseleva, and D. Noble, *Exp. Physiol.* **79**, 943 (1994). doi:10.1113/expphysiol.1994.sp003819
- [21] R. A. Duquette, A. Shmygol, C. Vaillant, A. Mobasheri, M. Pope, T. Burdyga, and S. Wray, *Biol. Reprod.* **72**, 276 (2005). doi:10.1095/biolreprod.104.033506
- [22] E. Jahn, I. Classen-Linke, M. Kusche, H. M. Beier, O. Traub, R. Grummer, and E. Winterhager, *Hum. Reprod.* **10**, 2666 (1995). doi:10.1093/oxfordjournals.humrep.a135764
- [23] W. C. Tong, C. Y. Choi, S. Karche, A. V. Holden, H. Zhang, and M. J. Taggart, *PLoS ONE* **6**, e18685 (2011). doi:10.1371/journal.pone.0018685
- [24] B. V. Safronov, M. Wolff, and W. Vogel, *Biophys. J.* **78**, 2998 (2000). doi:10.1016/S0006-3495(00)76838-X
- [25] J. M. Bekkers and M. Häusser, *Proc. Natl. Acad. Sci. USA* **104**, 11447 (2007). doi:10.1073/pnas.0701586104
- [26] G. J. Gutierrez, T. O'Leary, and E. Marder, *Neuron* **77**, 845 (2013). doi:10.1016/j.neuron.2013.01.016

## SUPPORTING INFORMATION FOR

### Spontaneous generation of persistent activity in diffusively coupled cellular assemblies

#### LIST OF SUPPLEMENTARY FIGURES

1. Decision tree to identify the dynamical state of a system of coupled excitable cells described by the FitzHugh-Nagumo model, each of which are coupled to a variable number of passive cells (EP model).
2. Decision tree to identify the dynamical state of a heterogeneous system of coupled cells described by the FitzHugh-Nagumo model, some of which are in the oscillatory regime, with the remaining ones in the excitable regime (OE model).
3. Differential sensitivity to small perturbations in a system of three coupled excitable cells, each attached to a variable number of passive cells, that displays coexistence of chaotic and non-chaotic activity for  $C_r = 0.19$  and  $D = 0.02$ , as described in the main text.
4. Time-evolution of the activation variables for two nodes coupled to each other in the EP model and the OE model, showing the absence and presence, respectively, of exact synchronization, and the spontaneous generation of activity in the OE model.
5. Comparison of spatio-temporal evolution of the activity in two-dimensional systems of the EP model and the OE model.

#### IDENTIFYING THE COLLECTIVE DYNAMICAL STATES OF THE MODELS

To characterize the various spatiotemporal patterns of collective dynamics that are observed in the models investigated in the main text, we measure several order parameters to aid in distinguishing the states. This is done with the help of the decision trees shown in Fig. S1 (for the EP model) and Fig. S2 (for the OE model). At each numbered decision point, threshold values  $\delta_{1,\dots,7}$  (Fig. S1) or  $\epsilon_{1,\dots,4}$  (Fig. S2), whose numerical values are indicated in the respective captions, are used to determine the answer to the corresponding question.

For the EP model comprising  $N$  coupled nodes (Fig. S1), where the order parameters are calculated using the time-series  $Y_i(t)$  representing the activation variable  $V_e$  of  $i$ -th node ( $i = 1, \dots, N$ ), the questions asked at the different decision points are:

1. Is there temporal variation in  $Y$ ? In practice, we measure the dispersion of each time-series  $Y_i$  and check if the average of this quantity over the nodes is greater than a threshold  $\delta_1 \ll 1$ . If true, at least one of the nodes is oscillating; else, the nodes are in time-invariant states.
2. If the nodes are in a time-invariant state, are the values of  $Y_i$  identical for all  $i$ ? In practice, we calculate the dispersion of the mean of the time-series across the nodes and check if it exceeds a threshold  $\delta_2 \sim 0$ . If true, it indicates that at least some of the  $Y_i$  are different, which characterizes an Inhomogeneous Steady State (ISS); else, all  $Y_i$  are the same indicating that it is an Oscillator Death (OD) state.
3. If there is temporal variation in  $Y$ , are all nodes oscillating? In practice, we check if the smallest dispersion of  $Y$  calculated for all nodes is greater than a threshold  $\delta_3 \ll 1$ . If not satisfied, it implies that at least one of the nodes is not oscillating and hence the state corresponds to a Chimera (Ch).
4. If all nodes are oscillating, do they all the same frequency? In practice, we check if the dispersion of the oscillation frequencies is greater than a threshold  $\delta_4 \sim 0$ . If true, then it corresponds to nodes having distinct frequencies which characterizes the Cluster Synchronization (CS) state.

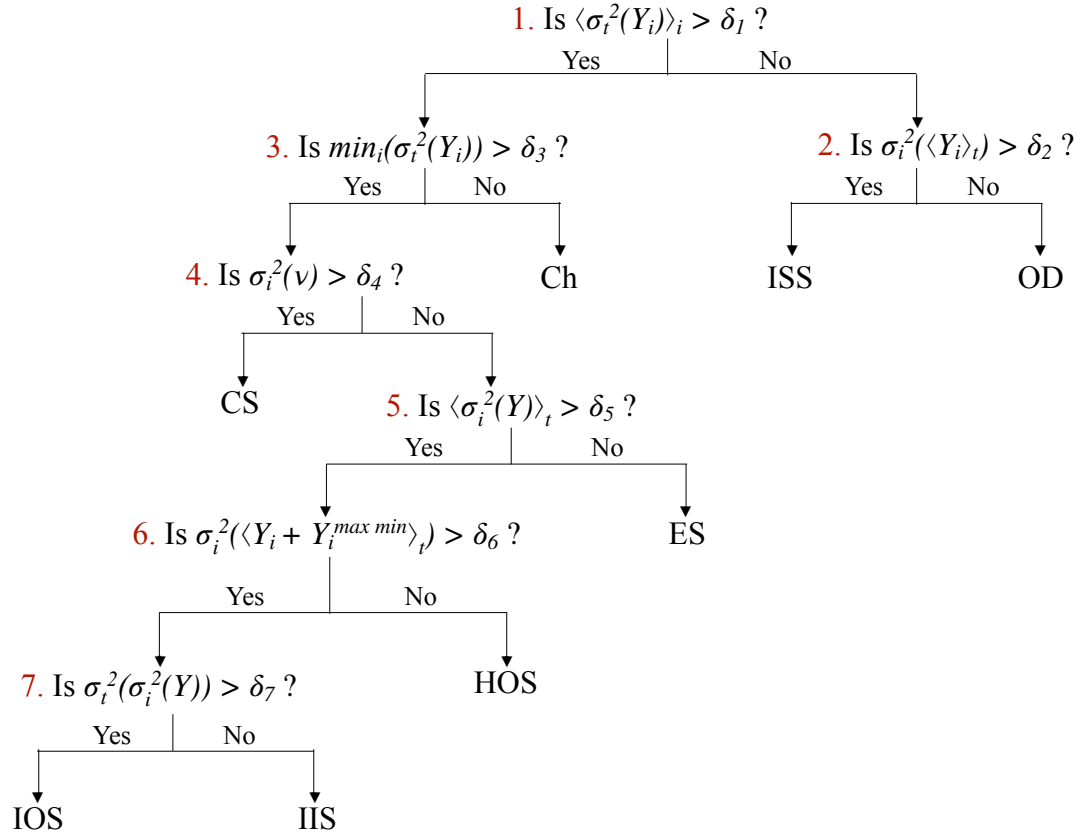


FIG. S1. Decision tree to identify the dynamical state of a system of coupled excitable cells described by the FitzHugh-Nagumo model, each of which are coupled to a variable number of passive cells (EP model). The order parameters used for determining the nature of the spatio-temporal pattern observed include the dispersions calculated across space [ $\sigma_t^2(\cdot)$ ], or across time [ $\sigma_t^2(\cdot)$ ], for the state variables  $Y_i$  ( $i = 1, \dots, N$ ) or the oscillation frequencies  $\nu$ . Averages calculated over space and over time are denoted by  $\langle \cdot \rangle_i$  and  $\langle \cdot \rangle_t$  respectively, while the deviation of the lowest value of the state variable for any node from its maximum calculated across space is denoted by  $Y_i^{\max \min} = \max_i(\min_t(Y_i)) - \min_t(Y_i)$ . The threshold values used to distinguish between the different states, viz., Oscillation Death (OD), Inhomogeneous Steady State (ISS), Chimera (Ch), Cluster Synchronization (CS), Exact Synchronization (ES), Homogeneous Out-of-phase Synchronization (HOS), Inhomogeneous In-phase Synchronization (IIS), and Inhomogeneous Out-of-phase Synchronization (IOS), are:  $\delta_1 = 10^{-3}$ ,  $\delta_2 = 10^{-5}$ ,  $\delta_3 = 10^{-3}$ ,  $\delta_4 = 10^{-7}$ ,  $\delta_5 = 10^{-5}$ ,  $\delta_6 = 10^{-7}$ , and  $\delta_7 = 10^{-4}$ .

5. If all nodes are oscillating at the same frequency, are they oscillating in phase? In practice, we measure the instantaneous dispersion between the amplitudes of the different nodes and check if its temporal average exceeds the threshold  $\delta_5 \sim 0$ . If it does not, the state corresponds to Exact Synchronization (ES) (belonging to the broader category of coherent states).
6. If the oscillators are not in phase, are their amplitudes the same? For this, we vertically displace each time series  $Y_i$  such that their minima  $\min(Y_i)$  are the same. We then calculate the dispersion in the amplitude and check if the difference is greater than the threshold  $\delta_6 \sim 0$ . If not, it corresponds to Homogeneous Out of phase Synchronization (HOS), where the oscillations have the same amplitude but are not phase synchronized (one of the two states that belong to the broader class of Global Synchronization).
7. If the oscillators have different amplitudes, are they phase synchronized? This can be determined by asking if the dispersion of  $Y$  calculated over the different nodes is invariant in time. In practice we calculate the dispersion of this quantity over time and check if it is greater than the threshold  $\delta_7 \ll 1$ . If not satisfied, then the nodes are synchronized in phase although oscillating with different amplitudes, corresponding to the state of Inhomogeneous In-phase Synchronization (IIS) (belonging to the broader category of coherent states); else,



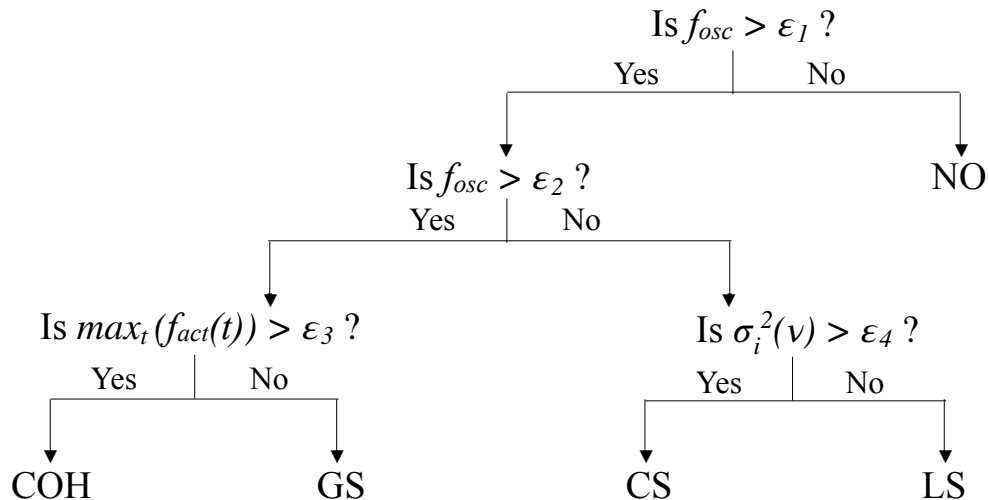


FIG. S2. Decision tree to identify the dynamical state of a heterogeneous system of coupled cells described by the FitzHugh-Nagumo model, some of which are in the oscillatory regime with the remaining ones in the excitable regime (OE model). The order parameters used for determining the nature of the spatio-temporal pattern observed include (i)  $f_{osc}$ : the number of oscillating nodes in the lattice, (ii)  $\max_t(f_{act}(t))$ : the maximum number of nodes that were active (i.e., above the excitation threshold  $\alpha$ ) together over the period of observation, and (iii)  $\sigma_i^2(\nu)$  is the dispersion of frequencies of all oscillating nodes calculated across space. The threshold values used to distinguish between the different states, viz., No Oscillations (NO), Cluster Synchronization (CS), Local Synchronization (LS), Global Synchronization (GS), and Coherence (COH), are:  $\epsilon_1 = 10^{-3}$ ,  $\epsilon_2 = 0.999$ ,  $\epsilon_3 = 0.995$  and  $\epsilon_4 = 10^{-10}$ .

the state is Inhomogeneous Out of phase Synchronization (IOS) (the other state that belongs to the broader class of Global Synchronization).

Note that we do not observe ES or HOS for the range of parameters used for the results reported in this paper.

For the OE model (Fig. S2), the questions asked in the different decision points are:

1. Is there a finite number of oscillating nodes in the system? In practice, we ask if the fraction of oscillating nodes  $f_{osc}$  is above a threshold  $\epsilon_1 \ll 1$ . If this is not satisfied, we classify the state as No Oscillations (NO).
2. Are all nodes oscillating? Again, in practice, we determine if  $f_{osc}$  is greater than a threshold  $\epsilon_2 \sim 1$ . If the answer is yes, we go on to ask if the oscillations are synchronized, while if the answer is no, we ask if the frequencies of the oscillating nodes are identical.
3. Are all the oscillating nodes synchronized in their phase? This is true if almost the entire set of nodes were simultaneously active (a node is considered to be active if its activation variable  $V_e$  is above the excitation threshold) and determined in practice by checking if the fraction of active nodes is larger than a threshold  $\epsilon_3 \sim 1$ . If true, then the states corresponds to Coherence (COH), else it is labeled as Global Synchronization (GS).
4. Are the frequencies of the oscillating nodes identical? We measure the dispersion of the frequencies and check if this is greater than a threshold  $\epsilon_4 \sim 0$ . If true, then the state is labeled as Cluster Synchronization (CS) characterized by the existence of many groups of oscillators having distinct frequencies; otherwise, the state is referred to as Local Synchronization (LS) in which all oscillating nodes have the same frequency.

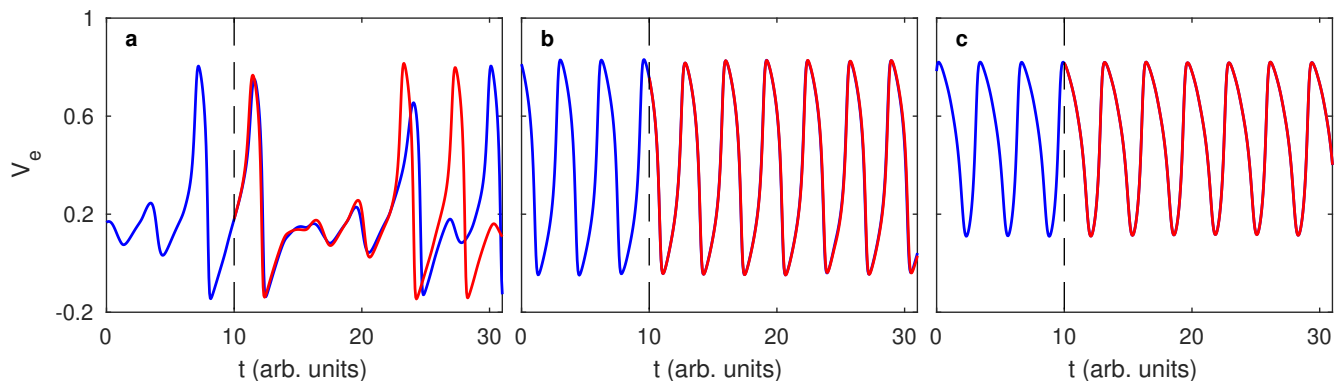


FIG. S3. Differential sensitivity to small perturbations in a system of three coupled excitable cells, each attached to a variable number of passive cells, which display coexistence of chaotic and non-chaotic activity for  $C_r = 0.19$  and  $D = 0.02$  as described in the main text [see Fig. 2]. Each cell is subjected to a perturbation of the same magnitude ( $= 10^{-3}$ ) applied at  $t = 10$  arb. units. While the cell exhibiting chaotic activity [panel (a)] displays exponential divergence of the perturbed trajectory (red) from the original one (blue), in the other two cells showing non-chaotic activity [panels (b) and (c)] the perturbed and original trajectories almost coincide.

### CHARACTERIZING THE COEXISTENCE OF CHAOTIC AND NON-CHAOTIC DYNAMICS IN A 3-NODE MOTIF OF THE EP MODEL

In the main text, we report the coexistence of chaotic and non-chaotic activity in a motif comprising 3 FHN nodes coupled to  $n_p = 1, 2$  and 3 passive cells respectively (see Fig. 2). We note that the usual method of demonstrating chaotic activity in a system is to show that its dynamics is sensitively dependent on initial conditions. In other words, two trajectories that begin from points that lie very close to each other in phase space will exponentially diverge with time. This is demonstrated in (Fig. S3) where the dynamical state of each unit is independently altered in turn by a very small magnitude perturbation and the subsequent time-evolution (shown in red) is compared with the trajectory of the node in the unperturbed system (shown in blue). As can be seen in panel (a), in the node exhibiting chaotic activity, the perturbed trajectory rapidly deviates from that observed in absence of perturbation, while for the other two nodes which display periodic activity, the perturbation does not result in any perceptible deviation [panels (b) and (c)]. The chaotic nature of the dynamics can be quantitatively established by noting that the maximal Lyapunov exponent (calculated by the TISEAN software) is positive.

### COMPARING THE COLLECTIVE DYNAMICS OBSERVED IN THE OE AND EP MODELS

In this subsection, we show that similar collective dynamical behavior is displayed by both models (Figs. S4 and S5). As both models use the FHN model to describe the individual excitable nodes, its parameters  $A$ ,  $\alpha$ ,  $\epsilon$  and  $k_e$  are kept the same in the two models such that it is a fair comparison. However, values for the distinct parameters in the two models, viz.,  $b$  in the OE model and  $C_r, n_p$  in the EP model, need to be suitably chosen such that a correspondence can be maintained between them. We note that for a given value of  $C_r$ , the resting state or the oscillation frequency of a node in the EP model depends on the value of  $n_p$ . On the other hand, in the OE model, it is the value of  $b$  which determines these. Thus, we can relate values of  $\{C_r, n_p\}$  with those of  $b$  that give rise to the same resting state or oscillation frequencies in the two models, respectively.

Fig. S4 (a) shows the time-series of the activation variable  $V_e$  for a pair of coupled excitable units in the EP model, one connected to  $n_p = 1$  passive cell (shown in blue) and the other to  $n_p = 2$  passive cells (shown in red). We observe that while the two are phase synchronized, their amplitudes are different. In the OE model shown in Fig. S4 (b), if we couple two FHN cells having distinct  $b$  values such that the coupled system has the same frequency as the EP model, we observe exact synchronization, as is evident from the complete overlap of the two time-series. Thus, not only are two nodes in the OE model phase synchronized (as is also the case in the EP model), they also have identical amplitudes (unlike in the EP model). Fig. S4 (c) shows the variation of the oscillation frequency  $\nu$  as a function of the coupling strength  $D$  between two FHN nodes having  $b = 0$  and 0.394, respectively, in the OE model.

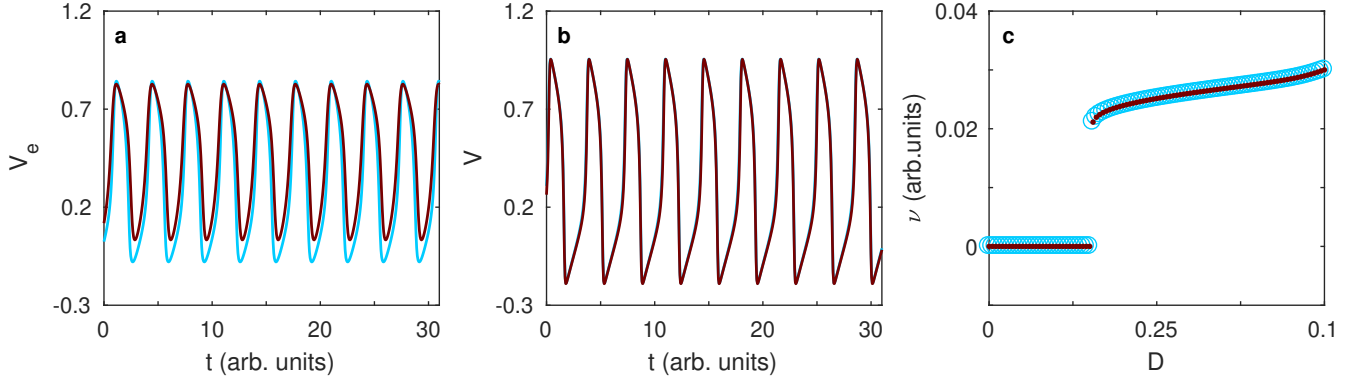


FIG. S4. Time-evolution of the activation variables for two nodes coupled to each other in (a) the EP model and (b) the OE model, showing the absence and presence, respectively, of exact synchronization. In (a), the two excitable cells are coupled to  $n_p = 1$  (blue curve) and  $n_p = 2$  (red curve) passive cells, respectively, with strength  $C_r = 0.4$  and interacting with each other with strength  $D = 0.2$ . In (b) the two cells differ in the numerical value of the FHN model parameter  $b$ , which are 0.2 and 0.181 respectively. (c) Oscillation frequencies for a system of two coupled excitable cells, each described by the FHN model but with distinct values for the parameter  $b$  ( $= 0$  and 0.394, respectively) such that they have very different steady states in isolation. The system is quiescent in the absence of any external stimulation until the coupling strength exceeds a critical value, when spontaneous periodic activity is observed.

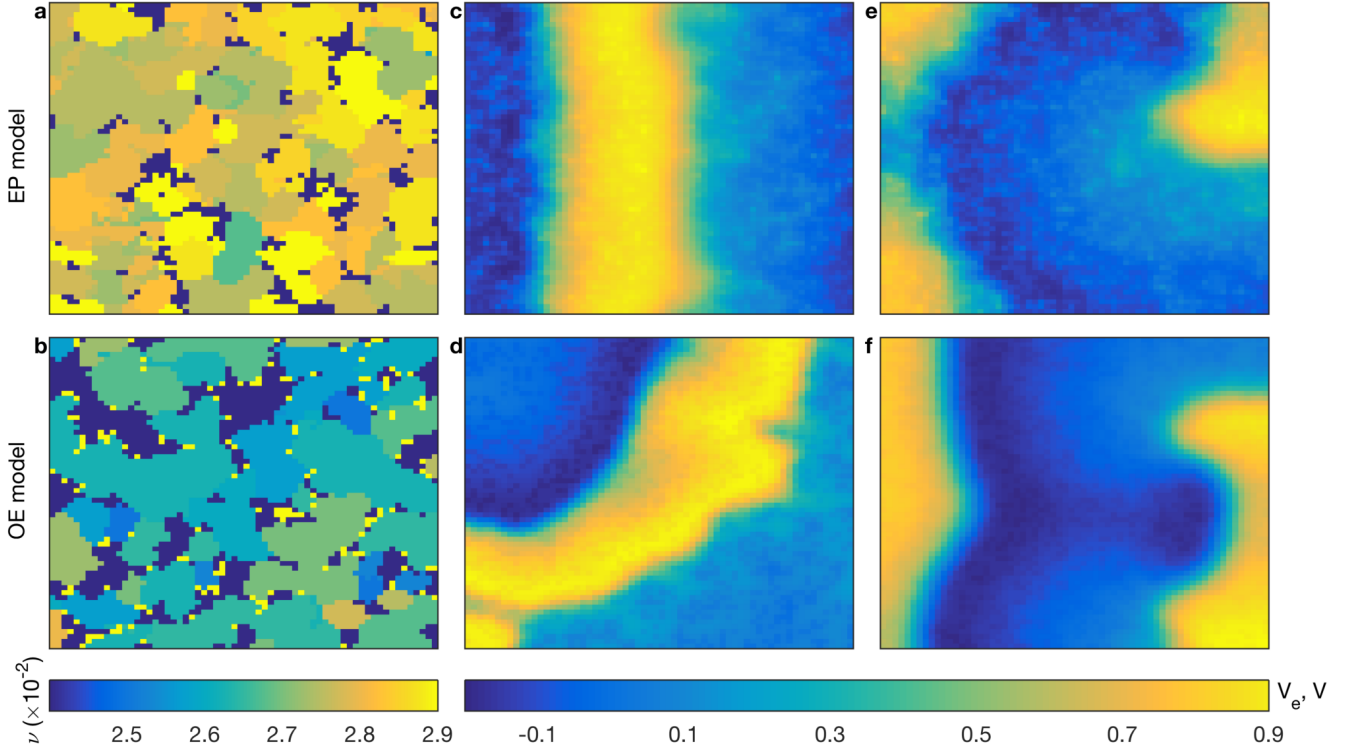


FIG. S5. Comparison of spatio-temporal evolution of the activity in two-dimensional systems of the EP model (top row,  $V_e$ ) and the OE model (bottom row,  $V$ ), showing similar behavior, viz., (a,b) cluster synchronization, as evident from the spatial distribution of frequencies  $\nu$ , (c,d) travelling wavefronts, and (e,f) spiral waves.

The uncoupled cells ( $D = 0$ ) do not show spontaneous oscillations - however, when they are coupled with a sufficient strength  $D$  they exhibit synchronized oscillations. The emergence of spontaneous oscillatory activity in the coupled system is similar to that reported for the EP model motifs in the main text [e.g., see Fig. 1 (j)].

We also observe similar dynamical regimes in the two models when considering a large number of coupled units arranged in two-dimensional lattices (Fig. S5). For instance, the collective dynamical states seen in the EP model, e.g., cluster synchronization (characterized by several groups such that the nodes in each are oscillating at a common frequency that is distinct from that of other groups) are also observed in the OE model [compare panels (a) and (b)]. Similarly, travelling wavefronts and spiral waves that are observed in the global synchronization regime in the EP model for annealed simulations [see panels (c) and (e)] are also observed in the OE model under suitable conditions [see panels (d) and (f)].